Robust watermarking based on modified Pigeon algorithm in DCT domain

Muath AlShaikh[1] · Malek Alzaqebah[2,3] · Sana Jawarneh[4]

Abstract

Watermarking is one of the techniques for improving the authenticity, integrity, and safety of data. A frequency domain approach is more robust against different attacks compared to a spatial domain approach. However, watermarking approaches are characterized by imperceptibility, robustness, and capacity. The problem of finding the optimal location for embedding the watermark can be challenging and affect the performance of the techniques, but it can also be seen as a path planning problem. Our main aim is to determine the optimal region for embedding the watermark in the Discrete Cosine Transform (DCT) based watermarking approach. We employ a modified Pigeon algorithm to determine the optimal embedding path, in which two objectives are considered to determine the optimal embedding place, as well as the behavior of the algorithm is enhanced to handle the nature of the problem. Our analysis indicates that our approach is highly resistant to different attacks, highly imperceptible after embedding the watermark, and consumes less complexity in embedding and extracting.

✉ Muath AlShaikh
m.alshaikh@seu.edu.sa

Malek Alzaqebah
maafehaid@iau.edu.sa

Sana Jawarneh
sijawarneh@iau.edu.sa

[1] Department of Computer Science, College of Computing and Informatics, Saudi Electronic University, 11673 Riyadh, Kingdom of Saudi Arabia

[2] Department of Mathematics, College of Science, Imam Abdulrahman Bin Faisal University, P.O. Box 1982, Dammam, Saudi Arabia

[3] Basic and Applied Scientific Research Center, Imam Abdulrahman Bin Faisal University, P.O. Box 1982, Dammam, Saudi Arabia

[4] Department of Computer Science, Applied College, Imam Abdulrahman Bin Faisal University, P.O. Box 1982, 31441 City of Dammam, Saudi Arabia

1 Introduction

With the fast advancement of technology, the Internet has emerged as the primary data carrier. It provides a fast, easy and low-cost channel. However, the integrity, authenticity and confidentiality issues for the data is still under attacks. It is very simple to modify and tamper the content. Therefore, many techniques have been proposed to guarantee and ensure the safety of content. Watermarking is one of the techniques for improving the authenticity, integrity, and safety of the content data. Watermarking is done either in spatial domain or frequency domain. The approaches in the frequency domain insert the watermark information into the coefficient of the original data. Discrete Fourier Transform (DFT) [29], Discrete Cosine Transform (DCT) [18], Discrete Wavelet Transform (DWT) [4], and Singular Value Decomposition (SVD) [12] are the most prominent frequency domain techniques. The approaches in the spatial domain embed the watermark immediately into the original image such as Least Significant Bit (LSB) [6, 20, 27].

Accordingly, any watermarking approach must be imperceptible, robust, and capable [5]. A watermark that is imperceptible implies high transparency, and that does not degrade after the watermark information has been embedded [3]. For copyright and authentication applications, robustness is crucial. By comparing the embedding space with the original data space, capacity factors measure how much space is needed for embedding. As a matter of fact, there is a tradeoff between these requirements and a good watermarking approach should satisfy them [19]. Therefore, the optimal places for embedding the watermark can be considered as path planning problem, Path planning problem deals with finding a feasible and optimal path from source to destination in such a way that some constraints are satisfied and maximized or minimized the objective function, thus an optimization algorithm to find the optimal path from a starting node to an ending node by transiting through several intermediate nodes is promising to solve the problem.

Swarm intelligence algorithms (SIAs) are optimization algorithms based on the collaborative behavior of individuals' that moving in a group (birds, fish, bees). The local and global search abilities of such algorithms have motivated researchers to use SIAs in many research areas in recent years. Among SIAs, the pigeon-inspired optimization (PIO) algorithm exposed good performance for optimization problems with some advantages such as: required few parameters [11], fast in processing [9], and less complexity [34].

PIO algorithm simulates the behavior of the real Pigeon, where the Pigeon is derived from "pipio" (a Latin word) which means the young cheeping bird. Researchers developed an air robot path planner based on the homing behavior of pigeons. To find food, the pigeons fly very long distances and use homing behavior by combining landmarks, the sun, and the magnetic field of the Earth to navigate [11].

In Pigeons, the compass and map process and landmark process are used for achieving homing behavior. The homing skills of the pigeon is believed to be based on the existence of very small magnetic particles that send signals to the brain located in its peak, making the pigeons capable of navigating to their home [30]. Pigeons can obtain a map and compass process by sensing the magnetic field of the earth and identifying their direction by observing the sun's altitude. Once the pigeons reach their destination, the Landmark process is applied, since the map and compass process will not work at this point.

Indeed, to find the optimal places for embedding the watermark using PIO algorithm, we divided an image to blocks, considering the starting block of an image left up block and the target block the right bottom block and the objective to find the path between the starting block

and the target block. In addition, an evaluated fitness function is defined and used to search for optimal path. Also, an improved PIO algorithm is proposed to with some restrictions that uses the fitness function to find the optimal path.

However, a watermarking approach is presented in this paper based on the DCT transform. Although a modified pigeon algorithm has been investigated to obtain the optimal path, this approach aims to preserve the imperceptibility of the original image, provides high robustness versus various attacks, as well as has enough capacity for watermark data.

The primary contributions of this work can be concluded in the following points:

– Preserve the imperceptibility of the original image after embedding with high fidelity.
– Provide a high robustness watermarking approach against various attacks.
– Achieve good balance between watermarking requirements.
– Provide watermarking approach with less computational complexity.

The remaining sections of the paper are organized as follows: the related works are stated and discussed in the second section. We present the proposed approach and the modified pigeon algorithm steps in the third section. Section four presents the experimental results. The fifth section presents the analysis of the proposed approach, and the sixth section provides the main approach conclusion.

2 Related works

The purpose of this section is to present the relevant and related works related to our approach, which is to investigate optimization solutions algorithms and frequency domain approaches for watermarking field, especially in the DCT domain. Pigeon-Inspired Optimization (PIO) algorithm is applied successfully to solve number of optimization problems [10, 11, 28, 34]. In [14] the author compared the performance of PIO algorithm with Dijkstra's Algorithm to discover the shortest path between two given nodes, where a conditional probability was used to choose the shortest path by pigeons, objective function was to maximizing the value of the f(x), where the value of f(x) is increased for each pigeon with shortest distance from the food, as results the solution given by PIO algorithm was comparable with the solution produced by using Dijkstra's Algorithm the solution provided an acceptable path but the maximization value of the objective function is not perfect. In [11] the authors solve the problem of air robot path planning using the PIO algorithm, the authors have proposed the mathematical model of PIO algorithm with detailed implementation. and the results proven to be efficient in improving the convergence speed, and good in global search.

In 2017, Zhang and Duan [34] presented predator prey pigeon inspired optimization in dynamic surroundings. The path planning for oilfield inspections has been solved by using the PIO, the PIO algorithm is modified to solve the problem of path planning for dynamic environment of three-dimensional oilfields in [13], where the authors defined a cost function for the optimal path searching.

A new feature selection algorithm based on pigeon inspired optimizer proposed by [2]. The proposed PIO for feature selection used to minimize the number of selected features and maximizing the prediction accuracy, the authors have proposed a cosine similarity method instead of using the sigmoid function for binarizing, resulting in increasing the convergence speed of the PIO algorithm. PIO algorithm showed a good performance with some advantages such as: required fewer parameters, fast in processing and less complexity compared with other

swarm optimization algorithms [9, 11, 34]. Nevertheless, the convergence speed of the PIO should be balanced, because the fast convergence is vulnerable for premature convergence [22].

Based on discrete cosine transforms and discrete wavelet transforms, [1] presented a robust watermarking method. To the DCT coefficients of each color component, DWT is utilized at one level for the original image. DWT bands at each color component of the original image are embedded with the DCT watermark transformed from the original. However, the approach provided a good robustness, but the capacity is too small. An algorithm for robustly watermarking medical images using discrete stationary wavelet and discrete cosine transforms (SWT-DCT) is presented in [8]. To extract and embed the watermark, the visual feature vector of the medical image was extracted using SWT-DCT. Also, to enhance the security of watermark information, it tampered with the watermark using a chaotic map. This combination of zero watermarking has allowed to create a watermark that will not be compromised by conventional attacks or geometric attacks. Even though the approach provided a good level of robustness, it also affected the imperceptibility of the origin data. The work in [23] presented a novel strong watermarking approach depending on lifting wavelet transforms (LWT) and discrete cosine transforms (DCT). The main gap in this approach is high computational complexity consuming.

To authenticate identity, signature watermarks and characters from patient reports are embedded into medical images. Additionally, before embedding into the host image, the watermark was encrypted with message digest (MD5) and the patient report was encoded with BCH error correcting code. The work [31] suggested a robust and blind watermarking algorithm for vector geographic data based on coordinate mapping and matching detection technologies. It was analyzed first how to resist data translation using matching detection and quantization index modulation (QIM). In addition, coordinate mapping, QIM, and matching detection algorithms were developed to watermark vector geographic data. The approach. Authentication and integrity purposes were met with this approach, but robustness was not considered.

A robust watermarking technique is presented in [24] that considers the DCT and SVD domains and uses a chaotic *kbest* gravitational search algorithm (CKGSA). The watermark is integrated into the principal component (PC) of the original image rather than the singular value because of eliminating the false positive problem. The use of CKGSA helps to balance robustness and imperceptibility by optimizing multiple embedding factors. Increasing the security and robustness of the watermarked image is achieved using the Arnold transform (AT). [25] uses the chaotic *kbest* gravitational algorithm and proposes an optimized robust watermarking approach. In order to obtain optimal embedding factors, they apply the chaotic *kbest* gravity search algorithm. [35] proposed a robust watermarking approach to maintain the integrity and security of medical images based on regions of interest (ROI) and integer wavelet transform (IWT) to authenticate and recover from damaged medical images. An image of a medical problem is split into two parts: (i.e., interest part and non-interest part). Following this, the integrity of ROI is validated by the hash algorithm, also the ROI data recovery is calculated simultaneously. Furthermore, a logistic chaotic map encryption algorithm is used to encrypt binary images with basic patient information, followed by the application of IWT transform to embed a synthetic watermark in the medical image. Despite the robustness of the above approaches, they failed to balance the other watermarking attributes, such as capacity, imperceptibility, and complexity.

Coefficients of the discrete cosine transform are used in [21] to develop a robust and blind watermarking procedure. A watermark enables the absolute differences between discrete cosine transform coefficients to be grouped together based on the watermark. The authors built a bimodal structure through modulating the shape of the absolute difference histogram. Adaptive thresholds are calculated using iterative selection methods in the extraction process. The approach served the blind watermarking aspect, but the retrieved watermark quality is very poor.

The work in [15] presented a method for watermarking medical images using the Wavelet Fusion (WF), Singular Value Decomposition (SVD). A discrete wavelet transform combined with scrambling methods are then applied to secure the watermarks (M-DWT). Multiple levels of security can be provided using the proposed approach by many applications including military applications, copyright protection, and telemedicine. This approach involves the merging of two digital watermarks into one in order to increase the embedding information payload. Utilizing the Arnold and Chaotic methods, the fused watermark is then scrambled. Final step is to embed the fused watermark in the cover image based on the three-level DWT and SVD methods. Watermark encryption is performed using the Arnold and chaotic algorithms due to their robustness, that increase the security and withstand various kinds of multimedia attacks. According to simulation results, the proposed system improves the quality while improving the capacity of embedded medical watermarks.

To hybridize the DWT, SVD, and DCT, a blind watermarking procedure is proposed in [7]. After encrypting the watermark image using the Arnold map, DCT and DWT are applied to the problem and to the host image, and then the SVD is applied. The watermark images are then embedded into the host images to create watermarked images. Singular Value Decomposition (SVD), Lifted Wavelet Transform (LWT), and Discrete Cosine Transform (DCT) were used for digital image watermarking in [33]. Using LH3 and LWT, decompose the host color image. LL3 sub bands of the third level LWT are transformed using DCT and SVD. Before embedding the image watermark (logo) into the LH3 sub band, the MD5 hash method is applied to strengthen its security. The information (Text watermark) now is more robust through Hamming error-correction code. By applying error-correcting code, the watermark length can be increased using arithmetic coding for lossless compression.

Particle Swarm Optimization (PSO) combined with kernel extreme learning machine (KELM) to watermark multi-spectral images; a novel copyright protection technique is presented in [26]. Based on local textures, host image blocks are selected that do not overlap. In the next step, discrete cosine transform (DCT) is applied to these selected blocks. To form the dataset, coefficients are scanned in zig-zag fashion in order to scan in a row-by-row fashion. By applying a regression approach, KELM predicted the outcome of a given input vector. A vector containing the watermark bits is then created. The PSO technique uses nature-inspired meta-heuristics to optimize scaling factors for the insertion of copyright logos into the original photos.

3 Proposed approach

In this section, we demonstrate the proposes watermarking approach based on modified pigeon algorithm in Discrete Cosine Transform (DCT). This approach aims to enhance the robustness of the DCT domain based on the modified pigeon algorithm. However, the proposed watermarking approach comprises of applying modified pigeon algorithm, embedding and

extraction phases. In the modified pigeon phase, we extracted the optimal embedding path from the original image, whereas in the embedding phase, we apply the modified pigeon algorithm to find the optimal path, next we embed the watermark in the DCT coefficient of the selected blocks. In the phase of extraction, the watermark is extracted non blindly from the attacked watermarked image. In the following section, we explain these phases in details.

In pigeon optimizer phase, the intelligent behavior of pigeons is utilized in searching for the optimal path for embedding the watermark of a given image's blocks, Pigeon Inspired Optimization (PIO) algorithm is a Swarm intelligence method, that simulates the social organisms of birds in learning the optimal path of finding the food sources. PIO uses a mathematical model to improve the solutions by the natural behavior of pigeons.

3.1 Original Pigeon algorithm

The original PIO algorithm uses the idea of map-compass and landmark processes, which converges very fast and possible to getting stuck in local optimal path. Moreover, PIO is a new bio-inspired swarm intelligence algorithm [11].

PIO algorithm involves two processes. These two processes of pigeon homing are mathematically represented by iteratively changing the positions and velocities of the birds. They are represented as, X_p is the position and V_p is the velocity of pigeon p, the new values of V_p and X_p are calculated at iteration i using Eqs. 1 and 2.

$$V_p = V_p(i-1) \cdot e^{-Ri} + Random \cdot (X_{glb} - X_p(i-1)) \tag{1}$$

$$X_p(i) = X_p(i-1) + V_p(i) \tag{2}$$

Where i-1 is the previous iteration and R is a factor of map and compass, *Random* is a randomly generated number in range [0, 1], and X_{glb} is the global best position obtained so far, X_{glb} can be found by comparing all pigeons' positions. Figure 1 illustrates the process of map and compass, where all pigeons follow the best pigeon's position, where all the positions are evaluated by an objective function to distinguish between the pigeon's positions.

As shown in Fig. 1, the best pigeon is signified by right centered pigeon's position and other pigeon will follow the best pigeon based on Eq. 1, where the straight (solid) arrow represents the first part of the Eq. 1, which is the present pigeon's path, the dashed arrow
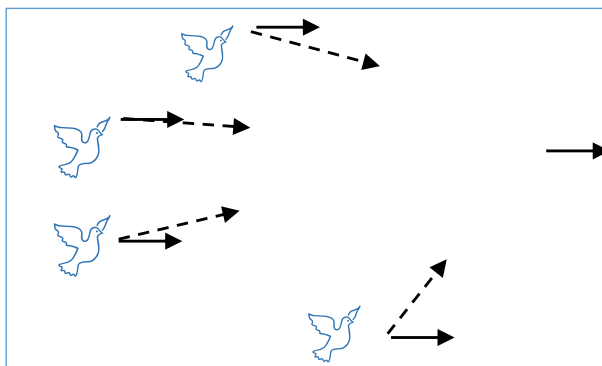
Fig. 1 Map and compass process of PIO, pigeons follow the best pigeon

represents the second part of the Eq. 1, it denotes the path that follows of the best pigeon. The vector summation of the two parts (arrows) represents the next flying direction [11]. Landmark process updates the number pigeons at each iteration using Eq. 3 where *Npigeons* is the new number of pigeons and *i* is the iteration number.

$$Npigeons(i) = \frac{Npigeons(i-1)}{2} \tag{3}$$

According to Fig. 2, the center pigeon in the circle represents the desired position of the pigeons. Equation 4 determines the position of half of the pigeons (in the circle, see Fig. 2), which adjust their path to the desired destination using Eq. 5 [2].

$$X_c(i) = \frac{\sum X_p(i) \cdot fitness(X_p(i))}{Npigeons \sum fitness(X_p(i))} \tag{4}$$

$$X_p(i) = X_p(i-1) + Random \cdot (X_c(i) - X_p(i-1)) \tag{5}$$

3.2 Modified Pigeon algorithm

The modified PIO considers for one source and one destination that can be used to find the optimal path for embedding a watermark into the image's blocks. We propose two objectives to find the optimal path, which are, the minimum total intensity of blocks between source and destination, and a minimum number of visited blocks.

The proposed two objectives can be explained by considering the image in Fig. 3 has starting block S and destination block D, where S, D ∈ k blocks set {*B0, B1,., Bk*}, and the parameters i.e., number of selected blocks and image intensity, the target is to find a set of
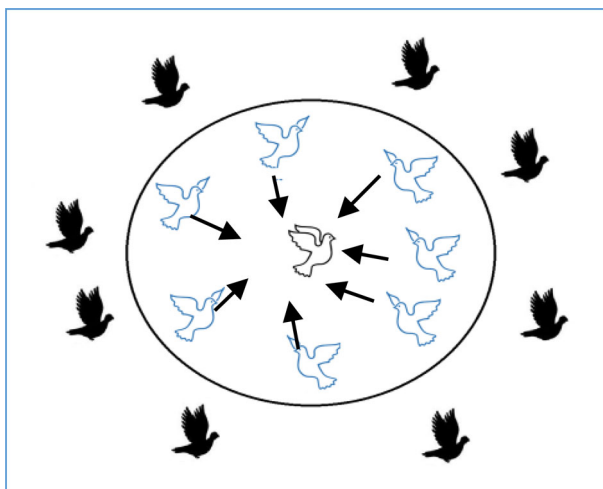
Fig. 2 Landmark process of PI

blocks $\{BP0, BP1,...,BPn, BPn + 1\}$ with $BP0 = S$ and $BPn + 1 = D$ such that satisfying all constraints and minimize as possible the objective function [34].

The objective function can be represented as:

$$F = w1*\frac{SB}{NB} + w2*\frac{1}{Mint} \tag{6}$$

where $w1$ and $w2$ are weight coefficients, which have relations to number of selected blocks (SB) over the total number of blocks (NB), and image mean intensity (Mint) separately in which $w1 + w2 = 1$.

Additionally, some constraints must be satisfied, such as: all selected blocks must be adjacent, each block must be visited exactly once, and starting block S is the first block and destination D is the last. Modified PIO assumes all pigeons are in Block S and food is in Block D (see Fig. 3). All blocks between S and D are used as landmarks. The implementation steps of the modified PIO algorithm can be summarized as follow:

Step1: Initialize the PIO parameters including the number of pigeons (Npigeons), the factor of map and compass (R), the total number of iterations used for map-compass process (maxIter_MC), and the total number of iterations used for landmark process (maxIter_L where maxIter_MC < maxIter_L).

Step2: Randomly initialize the population of Npigeons.

Step3: perform the map-compass process.

　　Step3.1: Calculate objective function using Eq. 6 for each pigeon then find the global best solution (X_{glb}).

　　Step3.2: Use Eqs. 1 and 2 to update the pigeon's paths and velocities then check if the paths respecting all constraints, if not repair the path.

　　Step3.3: Evaluate Pigeons using Eq. 6 and update the best Pigeon (X_{glb}),

　　Step3.4: map-compass process will be repeated maxIter_MC times (Steps 3.1 to 3.3).

Step4: Perform landmark process.

　　Step4.1: ranked all pigeons then keep the top half of pigeons.

　　Step4.2: Use Eq. 4 to find the position of the centered pigeon (the destination).

　　Step4.5: Use Eq. 5 to compute the new values of pigeons then update the pigeon's paths and the global best solution (X_{glb}).

　　Step4.6: landmark process will be repeated maxIter_L times starting from the deferent between maxIter_L and maxIter_MC + 1 (steps 4.1 to 4.5).

Step5: Output the global best solution (X_{glb}).

Moreover, the pseudocode of the modified PIO algorithm is shown in Fig. 4.

As shown in Fig. 4, the process of PIO consists of three parts. The first part concerns initializing PIO algorithm parameters, including the size of the population Npigeons, Map and Compass function, R, and the maximum number of iterations for Map and Compass and Landmark, where maxIter_L > maxIter_MC. Then, set a random velocity and path for each pigeon, calculate their objective function, and compare to find the best path. In the second part, we perform the map and compass process. It starts by updating the velocity and path using Eqs. 1 and 2, along with updating the best path. In the third part, pigeons are ranked based on their fitness values, which is the foundation of the landmark process. According to Eq. 3, half

Fig. 3 Image blocks

of the pigeons with low fitness values will follow the pigeons with high fitness values. A center for each pigeon (desirable destination) is calculated by using Eq. 4. In addition, all pigeons will change their flight direction in accordance with Eq. 5 based on the destination.

3.3 Embedding phase

The original image is divided into blocks of 80 by 80 pixels, then we apply the modified pigeon algorithm to obtain the optima path as we discussed in the previous phase, after that we convert the selected blocks into DCT-II transform. Subsequently, we embed the watermark information in the coefficient of the DCT information for each selected block, then stratify the inverse DC to obtain the original watermarked image. The embedding steps are summarized in the following steps:

```
Initialization
    Set Npigeons: number of pigeons
    Set D: dimension image blocks
    Set R: factor of map and compass
    Set Searchrange: the set of possible blocks, respecting all constraints
    Set maxIter_MC: total number of iterations used for map-compass process
    Set maxIter_L: total number of iterations used for landmark process
    set Xp: is the initial pigeon's paths
    set Vp: is the pigeon's velocities
    Calculate objective function of pigeon's paths
    Find the best path: Xglb

Map and compass Process
    For(Nc:1 until maxIter_MC)
        For(i:1 until Npigeons)
            while (Xpi not in search region)do
                use Equations 1 and 2 to find Vpi,Xpi
            endwhile
        endfor
        assess and update(Xp and Xglb)
    endfor

Landmark Process
    For (Nc:maxIter_MC+1 until maxIter_L)
        While(Xp not in search region)do
            all pigeons are ranked
            Npigeons = Npigeons /2
            keep the top half of pigeons
            Equation 4 to find Xc the position of the centered pigeon.
            Use Equation 5 to compute Xp
        endwhile
        update(Xp and Xglb)
    endfor
    Xglb :The global best solution as output
```

Fig. 4 Pseudocode of PIO algorithm

1- Divide the image (i) into non overlapping blocks (ib_k).
2- Apply the modified pigeon algorithm to obtain the optimal path (x_n) (Phase 3.1).
3- Convert the selective blocks into DCT-II coefficient

$$DCT_k = \sum_{n=0}^{N-1} x_n cos\left[\pi/N\left(n+\frac{1}{2}\right)k\right] \tag{7}$$

where DCT_k is the DCT-II transform coefficient of the block k, N is a number of the blocks

4- Insert the watermark logo in every transformed selective blocks based on the following equation

$$DCT_{wk} = (1-\beta)w + \beta*i_k = w + \beta(DCT_k - w) \tag{8}$$

Where DCT_{wk} is the watermarked of the block k, $\beta \in (0,1)$, w is the watermark image, DCT_k is the DCT transform coefficient value of block k.

5- Apply inverse DCT-II (IDCT-II) for each block based on the following equation

$$DCT'_k = \left(\left(\frac{1}{2)*x_0} + \sum_{n=1}^{N-1} x_n cos\left[\frac{\pi}{N}n\left(k+\frac{1}{2}\right)\right]\right)*\frac{2}{N}\right) \tag{9}$$

where DCT_k^* is the inverse DCT-II of block k.

6- Combine the watermarked blocks to obtain the watermarked image.

$$i_w = \sum_{n=1}^{N} DCT_k^* + Y_n \tag{10}$$

Where Y_n is the original block.

Figure 5 illustrates the general embedding schema of our approach.

3.4 Extraction phase

The embedded watermark can be extracted effectively from the watermarked image. The extraction is done non blindly whereas the original watermark is required during the extraction phase. The extraction processes illustrate in the following steps:

1- Divide the attacked watermarked image (iw_a) into non overlapping blocks ib_k.
2- Convert the selective blocks which is obtained from pigeon algorithm to DCT-II ($DCTiw_{ak}$).
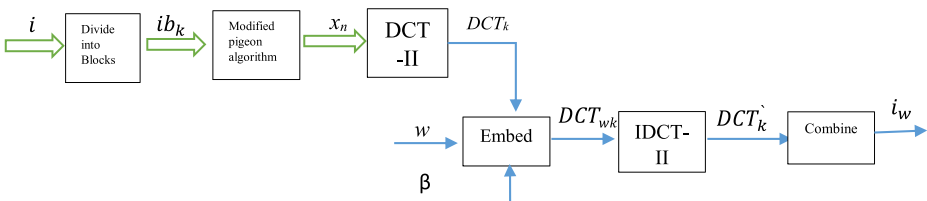
Fig. 5 Embedding schema

3- Extract the attacked watermark (w_a) for each selective blocks using the following equation:

$$w_{ak} = ((1 - \beta) * w_k - (\frac{1 - \beta}{\beta}) * DCTiw_{ak}) \tag{11}$$

Where w_{ak} is the extracted attacked watermark of the block number k, w_k is the original watermark and $DCTiw_{ak}$ is the attacked watermarked of block k

Figure 6 illustrates the extraction schema.

4 Experimental results

This section provides a performance analysis for our approach in order to prove the robustness and effectiveness of the approach. The approach is actualized in MATLAB R2017a with core i7 processor and 4 GB RAM.

Different grayscale images of size 400 by 400 pixels are considered in this work to measure the effectiveness of our approach, the watermark image is 80 by 80 pixels' size, we embed the watermark in each selective block. We will present three images (samples) for analysis and measurements purposes. Figure 7 illustrates the original image, watermark image and the watermarked images with different value of β = 0.1, 0.5, 0.7 and 0.98, respectively for the three selected images from the dataset.

As we can note from the previous figure, the watermark image can be inserted in the coefficient DCT for the selective blocks path with different value of β. When β is close to the 0, the watermark image is perceptible and effects on the watermarked image quality, while if the β is close to 1, the watermark image is imperceptible, and the watermarked image quality is very adequate.

4.1 Imperceptibility

One of the main requirements for any watermarking technique is to preserve the quality of the original image after embedding the watermark, which means that the watermarked image should be almost as the original image (imperceptible), at least by the human visual system.
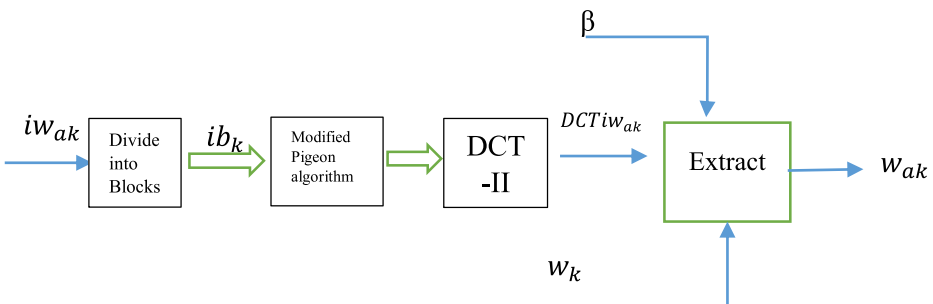
Fig. 6 Extraction schema
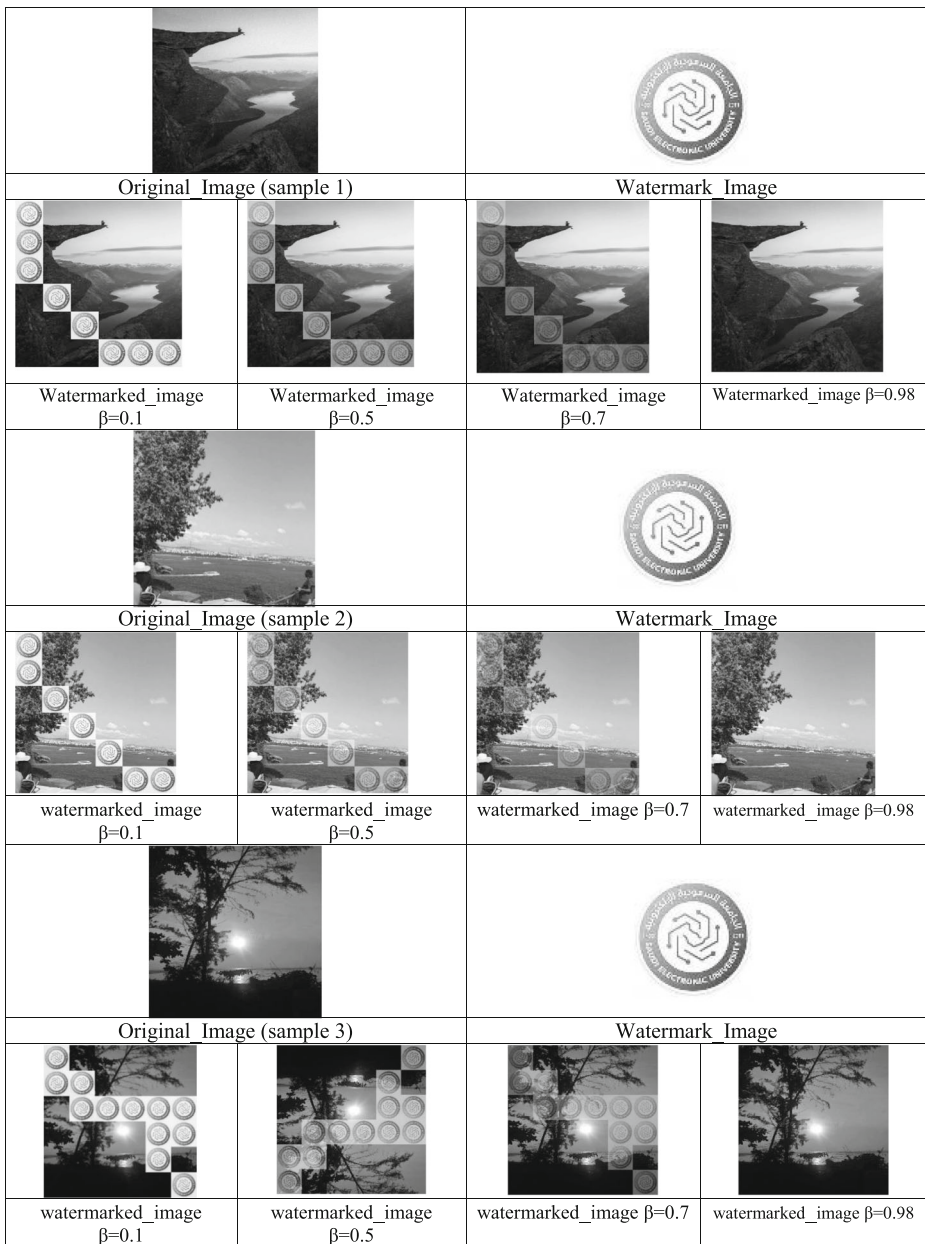
Fig. 7 Original, watermark and watermarked image for three selected images

Moreover, there is no degradation in the watermarked image by the embedding process. To measure the imperceptibility of the watermarking approach, we compare the original image by the watermarked image, one of the most popular measurements tools is Peak Signal to Noise Ratio (PSNR) [16]. Table 1 illustrates the PSNR measurements with different values of β for the three selected samples.

Table 1 indicates that the watermarked image quality is perfect when β is 0.98 which PSNR values achieve 57 dB. It means that the provided approach does not effect on the image quality and there is no degradation after embedding the watermark, as a result, the watermarked image is high transparency.

4.2 Robustness

Robustness refers to the ability to extract the watermark image from an attacked watermarked image. The approach is robust if the extracted watermark can be retrieved with a good quality. To test the robustness of our approach, we applied different geometric and non-geometric attacks on the watermarked images, then measured the PSNR, Structural Similarity Index (SSIM) [16], Normalize Correlation (NC) [32] and Bit Error Rate (BER) [17] between the original watermark and the extracted attacked watermark.

Table 2 presents JPEG with scaling factor of 60, PSNR of 60, Noise of scaling factor 60, rotation of 45-degree, median with scaling factor of 7 attacks on the watermarked image (sample 1), and their PSNR and SSIM values for the extracted watermark image.

In sample 1, we are embedding the watermark image in 8 positions, wa_1 signifies the extracted watermark in the first position, wa_2 signifies the extracted watermark in the second position, and so on. The average values of PSNR, SSIM, NC and BER in the case of JPEG attacks are 44.7654, 0.9978, 0.9829, 1.35% respectively. In case of PSNR attacks, the average values are 44.8765, 0.9974, 0.9832, 1.39%. In case of Noise attacks, the average value of PSNR is 43.3833dB, SSIM is 0.9944, NC is 0.9811 and BER is 1.63%. Rotation attacks have a PSNR of 39.1143dB, SSIM of 0.9876, NC of 0.9633 and BER of 2.62%. PSNR, SSIM, NC, BER are 43.643, 0.9977, 0.9783, 1.65%, respectively, in a median attack.

Presented in Table 3 are the sample 2 watermarked image with different attacks and the extracted watermarks along with their quality measurements.

The watermark image is embedded in seven locations in sample 2. For JPEG attacks, the average values of PSNR is 46.7654, SSIM is 0.9975, NC is 0.9788, BER is 1.45%. PSNR, SSIM, NC and BER for PSNR attacks are 47.3765, 0.9977, 0.9784, 1.41%, respectively. PSNR, SSIM, NC and BER are 43.3023dB, 0.9934, 0.9783, 1.46%, respectively, during noise attacks. In rotation attacks, the average values of PSNR, SSIM, NC and BER are 40.1803dB, 0.9876, 0.9704, 2.63%, respectively. In case of median attack, PSNR is 46.6170, SSIM is 0.9978, NC is 0.9794 and BER is 1.44%.

Table 1 PSNR measurements for three samples

Image	PSNR (dB)
Sample 1 with β=0.1	10.2073
Sample 1 with β=0.5	25.6456
Sample 1 with β=0.7	39.7345
Sample 1 with β=0.98	53.6113
Sample 2 with β=0.1	12.5467
Sample 2 with β=0.5	26.3865
Sample 2 with β=0.7	37.5689
Sample 2 with β=0.98	56.4563
Sample 3 with β=0.1	17.4534
Sample 3 with β=0.5	28.3325
Sample 3 with β=0.7	38.5833
Sample 3 with β=0.98	57.5453

Table 2 Sample 1 watermarked image with various attacks and the extracted watermark
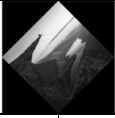
Attack type	Attacked watermarked image							
JPEG								
Wa	wa_1	wa_2	wa_3	wa_4	wa_5	wa_6	wa_7	wa_8
PSNR	46.3456	46.7654	47.0277	46.6578	46.4454	45.9565	44.2211	43.6744
SSIM	0.9944	0.9973	0.9972	0.9945	0.9971	0.9981	0.9910	0.9933
NC	0.9854	0.9854	0.97653	0.98611	0.9832	0.9795	0.9799	0.9694
BER	1.33%	1.64%	1.23%	1.54%	1.53%	1.59%	1.68%	1.74%
Extracted watermark								
PSNR								
Wa	wa_1	wa_2	wa_3	wa_4	wa_5	wa_6	wa_7	wa_8
PSNR	48.0328	44.7863	44.8387	44.5097	43.9994	43.8373	44.9063	43.4080
SSIM	0.9975	0.9974	0.9974	0.9974	0.9976	0.9975	0.9974	0.9976
NC	0.9843	0.9745	0.9752	0.9762	0.9701	0.9704	0.9702	0.9722
BER	1.36%	1.65%	1.63%	1.65%	1.73%	1.73%	1.66%	1.83%
Extracted watermark								
Noise								
Wa	wa_1	wa_2	wa_3	wa_4	wa_5	wa_6	wa_7	wa_8
PSNR	43.3834	43.3289	43.4466	43.3805	43.3816	43.3580	43.3391	43.3666
SSIM	0.9938	0.9940	0.9946	0.9944	0.9942	0.9942	0.9943	0.9941
NC	0.9744	0.9743	0.9735	0.9722	0.9734	0.9732	0.9743	0.9734
BER	1.45%	1.48%	1.48%	1.46%	1.46%	1.47%	1.49%	1.45%
Extracted watermark								
Rotation								
Wa	wa_1	wa_2	wa_3	wa_4	wa_5	wa_6	wa_7	wa_8
PSNR	39.9395	39.9393	37.4442	40.0833	36.1104	38.9568	41.9395	40.9395
SSIM	0.9878	0.9878	0.9875	0.9874	0.9877	0.9878	0.9878	0.9878
NC	0.9723	0.9725	0.9643	0.9734	0.9711	0.9657	0.9622	0.9643
BER	2.69%	2.69%	2.57%	2.56%	2.57%	2.63%	2.67%	2.69%
Extracted watermark								
Median								
Wa	wa_1	wa_2	wa_3	wa_4	wa_5	wa_6	wa_7	wa_8
PSNR	47.6326	43.2108	43.4989	42.9533	43.2592	43.0643	43.4353	42.9395
SSIM	0.9977	0.9977	0.9977	0.9978	0.9977	0.9977	0.9978	0.9978
NC	0.9855	0.9743	0.9734	0.9784	0.9792	0.9724	0.9793	0.9721
BER	1.24%	1.67%	1.66%	1.69%	1.63%	1.63%	1.64%	1.69%
Extracted watermark								

Table 3 Sample 2 watermarked image with various attacks and the extracted watermark
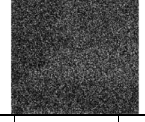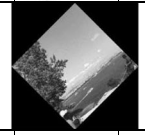
Attack type	Attacked watermarked image						
JPEG							
Wa	wa_1	wa_2	wa_3	wa_4	wa_5	wa_6	wa_7
PSNR	46.9945	46.5434	45.8435	47.7268	47.4229	47.0471	45.9609
SSIM	0.9974	0.9974	0.9973	0.9978	0.9978	0.9976	0.9975
NC	0.9744	0.9733	0.9711	0.9810	0.9821	0.9813	0.9723
BER	1.35%	1.36%	1.37%	1.32%	1.32%	1.33%	1.45%
Extracted watermark							
PSNR							
Wa	wa_1	wa_2	wa_3	wa_4	wa_5	wa_6	wa_7
PSNR	47.3626	47.1797	46.6613	47.5528	47.4137	47.2224	46.5571
SSIM	0.9975	0.9975	0.9975	0.9978	0.9978	0.9976	0.9976
NC	0.9822	0.9832	0.9810	0.9832	0.9842	0.9854	0.9792
BER	1.32%	1.32%	1.35%	1.43%	1.41%	1.46%	1.58%
Extracted watermark							
Noise							
Wa	wa_1	wa_2	wa_3	wa_4	wa_5	wa_6	wa_7
PSNR	43.4589	43.3975	43.3023	43.4365	43.4202	43.3097	43.3870
SSIM	0.9937	0.9939	0.9937	0.9932	0.9932	0.9935	0.9939
NC	0.9833	0.9745	0.9743	0.9783	0.9721	0.9711	0.9742
BER	1.65%	1.66%	1.69%	1.73%	1.59%	1.67%	1.66%
Extracted watermark							
Rotation							
Wa	wa_1	wa_2	wa_3	wa_4	wa_5	wa_6	wa_7
PSNR	39.9395	39.9393	40.5073	40.8059	42.2224	38.9395	38.9395
SSIM	0.9878	0.9878	0.9875	0.9875	0.9876	0.9878	0.9878
NC	0.9733	0.9753	0.9744	0.9775	0.9853	0.9694	0.9681
BER	2.74%	2.78%	2.54%	2.58%	2.34%	2.73%	2.77%
Extracted watermark							
Median							
Wa	wa_1	wa_2	wa_3	wa_4	wa_5	wa_6	wa_7
PSNR	47.2940	47.3058	46.6170	47.7572	47.4080	47.2962	46.2468
SSIM	0.9977	0.9978	0.9977	0.9978	0.9978	0.9978	0.9977
NC	0.9954	0.9894	0.9943	0.9921	0.9942	0.9893	0.9843
BER	1.45%	1.44%	1.47%	1.43%	1.42%	1.43%	1.49%
Extracted watermark							

Table 4 Sample 3 watermarked image with various attacks and the extracted watermark

Attack type	Attacked watermarked image											
JPEG												
Wa	wa_1	wa_2	wa_3	wa_4	wa_5	wa_6	wa_7	wa_8	wa_9	wa_{10}	wa_{11}	wa_{12}
PSNR	43.6544	43.6786	42.6557	44.5441	42.5543	46.5444	44.6567	46.2234	43.4567	44.8654	42.5833	45.6623
SSIM	0.9976	0.9980	0.9981	0.9979	0.9979	0.9982	0.9982	0.9981	0.9979	0.9978	0.9978	0.9980
NC	0.9766	0.9785	0.9788	0.9812	0.9796	0.9854	0.9823	0.9912	0.9865	0.9812	0.9744	0.9826
BER	1.67%	1.67%	1.78%	1.43%	1.77%	1.47%	1.46%	1.44%	1.57%	1.56%	1.87%	1.43%
Extracted watermark												
PSNR												
PSNR	45.7765	45.7623	45.3323	44.6785	47.5432	46.8432	45.5532	44.7255	43.7659	44.5578	44.7688	43.6224
SSIM	0.9987	0.9987	0.9985	0.9985	0.9883	0.9981	0.9982	0.9982	0.9979	0.9977	0.9980	0.9976
NC	0.9822	0.9812	0.9822	0.9801	0.9844	0.9832	0.9813	0.9799	0.9785	0.9788	0.9788	0.9743
BER	1.55%	1.55%	1.54%	1.65%	1.43%	1.34%	1.54%	1.62%	1.64%	1.60%	1.59%	1.76%
Extracted watermark												
Noise												
PSNR	43.4432	43.7654	44.7651	45.3323	43.7658	43.7232	43.8651	44.7654	42.6798	42.5672	43.6589	45.2456
SSIM	0.9943	0.9933	0.9943	0.9932	0.9965	0.9943	0.9943	0.9948	0.9931	0.9939	0.9945	0.9965
NC	0.9747	0.9743	0.9732	0.9799	0.9744	0.9785	0.9788	0.9783	0.9713	0.9743	0.9744	0.9821
BER	1.55%	1.54%	1.49%	1.32%	1.87%	1.79%	1.76%	1.65%	1.84%	1.82%	1.79%	1.44%
Extracted watermark												
Rotation												
PSNR	39.5543	39.9554	39.9395	37.9393	40.5073	40.8059	41.2224	38.9395	38.9395	38.9395	38.9393	39.6548
SSIM	0.9879	0.9880	0.9878	0.9878	0.9875	0.9875	0.9876	0.9878	0.9878	0.9878	0.9878	0.9878
NC	0.9686	0.9699	0.9653	0.9633	0.9746	0.9732	0.9811	0.9643	0.9655	0.9637	0.9636	0.9694
BER	2.74%	2.69%	2.67%	2.67%	2.34%	2.36%	2.22%	2.76%	2.77%	2.77%	2.79%	2.76%
Extracted watermark												
Median												
PSNR	44.6326	43.2108	43.4989	42.9533	43.2592	43.0643	43.4353	42.9395	42.8744	43.6326	45.4534	43.2254
SSIM	0.9978	0.9977	0.9977	0.9978	0.9977	0.9977	0.9978	0.9978	0.9978	0.9977	0.9983	0.9979
NC	0.9802	0.9801	0.9796	0.9734	0.9758	0.9786	0.9784	0.9712	0.9722	0.9734	0.9812	0.973
BER	1.53%	1.67%	1.66%	1.71%	1.69%	1.69%	1.68%	1.72%	1.73%	1.83%	1.59%	1.77%
Extracted watermark												

Here, the sample 3 watermarked image present in the Table 4 with 12 embedded locations.

Modified Pigeon algorithm provided 12 available locations in sample 3, the watermark image is embedded in them. For JPEG attacks, the average value of PSNR is 44.4654, SSIM is 0.9975, NC is 0.9801, BER is 1.61%. The PSNR, SSIM, NC and BER in case of PSNR attacks are 45.3765, 0.9975, 0.9807 and 1.53, respectively. During noise attacks, the PSNR, SSIM, NC and BER values are 43.3623dB, 0.9935, 0.9787 and 1.67% respectively. The average values of the PSNR, SSIM, NC and BER of rotation attacks are 39.8203dB, 0.9879, 0.9694 and 2.59%, respectively. In case of median attack, PSNR, SSM, NC and BER are 44.8755, 0.9978, 0.9798 and 1.67%, respectively.

It is obviously that the extracted watermark is obtained with high quality resolution, it means that the approach is robustness against attacks.

4.3 Complexity

It is important that the acceptable watermarking technique provides a good balance between the major watermarking requirements. The complexity of the watermarking process is a critical factor. In real time applications, we consider the less complex approach to be suitable. For evaluating our watermarking approach, we measured the time required for obtaining the path using the modified pigeon algorithm and the time required for embedding and extracting.

The following table presents the required time for define the optimal bath based on modified pigeon algorithm and the embedding and extraction time for the three samples comparing to the relative works [1] (DCT-DWT), [23] (LWT-DCT), [24] (DCT-SVD) and [21] (DCT-HIST). As we can note from this table, our approach consumes less time in define the path, embedding time and extracting time.

According to Table 5, the time required for the whole process for sample 1 is 1.194 s. In addition, the second sample required 1.007s, while the third sample required 1.466s. As we can note from this table, our approach consumes less time in define the path, embedding time and extracting time.

Table 5 The required time for the proposed approach

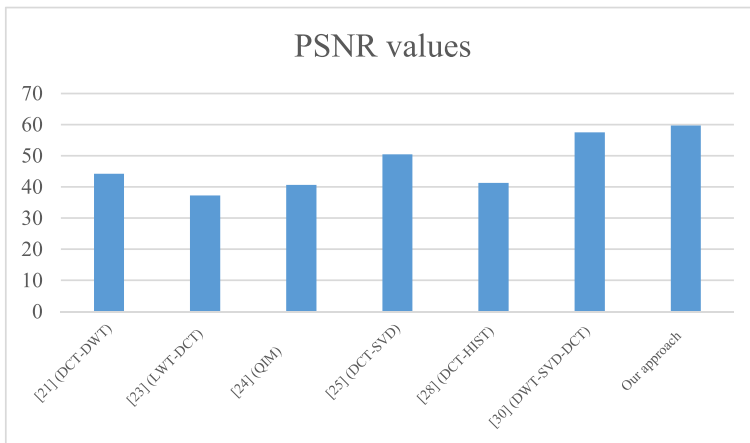| Image	Pigeon algorithm time (s) (Define the embedding place)	Embedding time (s)	Extraction time (s)
sample 1	0.496	0.388	0.310
sample 2	0.365	0.353	0.289
sample 3	0.584	0.523	0.359
[1] DCT-DWT	0.645	0.854	0.654
[23] LWT-DCT	0.467	0.546	0.743
[24] DCT-SVD	0.736	0.854	0.443
[21] DCT-HIST	0.538	0.734	0.543

Fig. 8 PSNR values of the watermarked image

5 Analysis of the proposed approach

A modified pigeon algorithm and DCT based frequency domain watermarking technique has been proposed to provide robustness and efficiency approach. In this way, the copyright issue is addressed. The proposed method achieves an acceptable PSNR with a robustness factor against most attacks. In Section 4.3, the computational complexity of the proposed approach is calculated. In addition, the imperceptibility factor is investigated, and we found that the proposed approach achieved very high values of the quality of the watermarked image. Hence, a comparative study of recent approaches will be presented. Comparing our work to others, we will focus on imperceptibility, robustness, and complexity.

Figure 8 presents the PSNR values of the watermarked image of our approach comparing with the works in [1] (DCT-DWT), [23] (LWT-DCT), [31] (QIM), [24] (DCT-SVD), [21] (DCT-HIST) and [7] (DWT-SVD-DCT).

The PSNR value of the proposed approach is around 57dB, and it is higher than recent approaches. Basically, the watermarked images have a high imperceptibility aspect, and the technique does not affect the quality of the cover image.

Our analysis study also examines robustness, the major attacks are JPEG compression, PSNR, Noise, Rotation and Median filter attacks. Table 6 illustrates the average values of the PSNR, SSIM, NC and BER for our approach comparing with other techniques.

According to Table 6, our approach produces better PSNR, SSIM, NC, and BER measurements. It indicates that the proposed approach is more resistant to various attacks than other techniques.

6 Conclusion

Watermarking using DCT was proposed in this paper. Modified Pigeon algorithm is used to determine the optimal embedding region. By applying the modified pigeon algorithm,

Table 6 Comparison of the robustness of the proposed approach with existing methods

Attacks type	Approaches	PSNR	SSIM	NC	BER
JPEG 60	[1] DCT-DWT	46.5345	NA	0.9556	NA
	[23] LWT-DCT	34.72	NA	0.9598	2.1%
	[24] DCT-SVD	45.332	0.9843	0.9654	1.83%
	[21] DCT-HIST	43.5442	0.9884	NA	1.65%
	Our approach	46.9233	0.9977	0.9856	1.54%
PSNR 60	[1] DCT-DWT	36.767	NA	0.9612	NA
	[23] LWT-DCT	35.67	NA	0.8284	2.15%
	[31] QIM	45.4432	0.9764	0.9673	NA
	[24] DCT-SVD	39.5543	0.9912	0.9755	2.43%
	[21] DCT-HIST	43.6643	0.9924	NA	4.53%
	[7] DWT-SVD-DCT	NA	NA	0.9956	NA
	Our approach	45.3765	0.9975	0.9801	1.61%
Noise	[23] LWT-DCT	36.01	NA	0.7935	3.54%
	[24] DCT-SVD	34.523	0.985	0.972	2.43%
	[21] DCT-HIST	38.4342	0.9924	NA	NA
	[7] DWT-SVD-DCT	37.3441	0.9547	0.9453	3.5%
	Our approach	43.3623	0.9935	0.9787	1.67%
Rotation	[1] DCT-DWT	NA	0.8642	0.6342	NA
	[23] LWT-DCT	28.51	NA	0.0367	49%
	[31] QIM	21.2	NA	0.654	NA
	[24] DCT-SVD	32.32	NA	0.784	NA
	[21] DCT-HIST	34.54	NA	NA	12.45%
	[7] DWT-SVD-DCT	37.44	0.9643	0.9987	NA
	Our approach	39.1143	0.9876	0.9633	2.62%
Median	[1] DCT-DWT	35.767	0.9034	0.8765	NA
	[23] LWT-DCT	36.01	0.7364	NA	6.29%
	[24] DCT-SVD	36.43	0.865	NA	NA
	[21] DCT-HIST	33.45	NA	NA	8.76%
	Our approach	44.8755	0.9978	0.9798	1.67%

we converted the cover image into a DCT transform, and then embedded the watermark logo in the obtained path from the modified pigeon algorithm. The watermarked image is then obtained by applying inverse DCT. We transformed the attacked watermarked image into a DCT transformation, then extracted the attacked watermark. Moreover, the approach is more robust, highly imperceptible, and requires less computational power.

References

1. Abdulrahman AK, Ozturk S (2019) A novel hybrid DCT and DWT based robust watermarking algorithm for color images. Multimed Tools Appl 78(12):17027–17049
2. Alazzam H, Sharieh A, Sabri KE (2020) A feature selection algorithm for intrusion detection system based on pigeon inspired optimizer. Expert Syst Appl 148:113249

3. AlShaikh M, Laouamer L, Nana L, Pascu AC (2015), November A novel robust informed watermarking approach and tamper detection based on weber differential excitation descriptor. In: 2015 International Symposium on Intelligent Signal Processing and Communication Systems (ISPACS). IEEE, pp 194–198

4. AlShaikh M, Laouamer L, Nana L, Pascu A (2016) A novel CT scan images watermarking scheme in DWT transform coefficients. IJCSNS 16(1):62

5. AlShaikh M, Nana L, Laouamer L, Christine A (2016) Formal concept analysis to improve robustness on medical image watermarking schemes in the spatial domain. Int J Comput Sci Inform Secur 14(2):261

6. AlShaikh M, Laouamer L, Laouid A, Bounceur A, Hammoudeh M, July (2019) Robust and Imperceptible Medical Image Watermarking Based on Dijkstra Algorithm. In: Proceedings of the 3rd International Conference on Future Networks and Distributed Systems, pp 1–6

7. Begum M, Ferdush J, Uddin MS (2021) A hybrid robust watermarking system based on discrete cosine transform, discrete wavelet transform, and singular value decomposition. J King Saud Univ Comput Inf Sci. https://doi.org/10.1016/j.jksuci.2021.07.012

8. Dai Q, Li J, Bhatti UA, Chen YW, Liu J (2019)SWT-DCT-based robust watermarking for medical image. Innovation in Medicine and Healthcare Systems, and Multimedia. Springer, Singapore, pp 93–103

9. Deng Y, Duan H (2016) Control parameter design for automatic carrier landing system via pigeon-inspired optimization. Nonlin Dyn 85(1):1–10

10. Deng Y, Duan H (2016) Control parameter design for automatic carrier landing system via pigeon-inspired optimization. Nonlinear Dyn 85(1):97–106

11. Duan H, Qiao P (2014)Pigeon-inspired optimization: A new swarm intelligence optimizer for air robot path planning. Int J Intell Comput Cybernetics 7(1):24–37

12. Gao Q, Xia W, Wan Z, Xie D, Zhang P (2020), April Tensor-SVD based graph learning for multi-view subspace clustering. In: Proceedings of the AAAI Conference on Artificial Intelligence, vol 34, no 04, pp 3930–3937

13. Ge F, Li K, Han Y, Xu W, Wang YA (2020) Path planning of UAV for oilfield inspections in a three-dimensional dynamic environment with moving obstacles based on an improved pigeon-inspired optimization algorithm. Appl Intel 50(9):2800–2817

14. Goel S (2014), September Pigeon optimization algorithm: A novel approach for solving optimization problems. In: 2014 International Conference on Data Mining and Intelligent Computing (ICDMIC). IEEE, pp 1–5

15. Hemdan EED (2021) An efficient and robust watermarking approach based on single value decompression, multi-level DWT, and wavelet fusion with scrambled medical images. Multimed Tools Appl 80(2):1749–1777

16. Hore A, Ziou D (2010), August Image quality metrics: PSNR vs. SSIM. In: 2010 20th international conference on pattern recognition. IEEE, pp 2366–2369

17. Jeruchim M (1984) Techniques for estimating the bit error rate in the simulation of digital communication systems. IEEE J Sel Areas Commun 2(1):153–170

18. Ko HJ, Huang CT, Horng G, Shiuh-Jeng WAN (2020) Robust and blind image watermarking in DCT domain using inter-block coefficient correlation. Inf Sci 517:128–147

19. Laouamer L, Muath A, Nana LT, Pascu AC (2015), September Improving authenticity and robustness of medical images watermarking schemes based on multi-resolution decomposition. In: Proceedings of the 12th IEEE International Conference on Imaging Systems and Techniques, pp pp-331

20. Laouamer L, Alshaikh M, Nana L, Pascu AC (2016) Generating optimal informed and adaptive watermark image based on zero-suppressed binary decision diagrams for medical images. Int J Electron Secur Digit Forensics 8(3):262–284

21. Li J, Zhang C (2020) Blind and robust watermarking scheme combining bimodal distribution structure with iterative selection method. Multimed Tools Appl 79(1):1373–1407

22. Pandey HM, Chaudhary A, Mehrotra D (2014) A comparative review of approaches to prevent premature convergence in GA. Appl Soft Comput 24:1047–1077

23. Singh AK (2019) Robust and distortion control dual watermarking in LWT domain using DCT and error correction code for color medical image. Multimed Tools Appl 78(21):30523–30533

24. Singh R, Ashok A (2021) An optimized robust watermarking technique using CKGSA in frequency domain. J Inform Secur Appl 58:102734

25. Singh R, Ashok A, Saraswat M (2020) Optimised robust watermarking technique using CKGSA in DCT-SVD domain. IET Image Proc 14(10):2052–2063

26. Sisaudia V, Vishwakarma VP (2021) Copyright protection using KELM-PSO based multi-spectral image watermarking in DCT domain with local texture information-based selection. Multimed Tools Appl 80(6): 8667–8688

27. Soni GK, Rawat A, Jain S, Sharma SK (2020) A pixel-based digital medical images protection using genetic algorithm with LSB watermark technique. Smart Systems and IoT: Innovations in Computing. Springer, Singapore, pp 483–492
28. Sun H, Duan H (2014) Pid controller design based on prey-predator pigeon-inspired optimization algorithm. In: 2014 IEEE international conference on mechatronics and automation. IEEE, pp 1416–1421
29. Sun XC, Lu ZM, Wang Z, Liu YL (2021) A geometrically robust multi-bit video watermarking algorithm based on 2-D DFT. Multimed Tools Appl 80(9):13491–13511
30. Varun A, Kumar MS (2018) A comprehensive review of the pigeon inspired optimization algorithm. Int J Eng Technol 7(329):758–761. https://doi.org/10.14419/ijet.v7i4.29.21654
31. Yang C, Zhu C, Wang Y, Rui T, Zhu J, Ding K (2020) A robust watermarking algorithm for vector geographic data based on Qim and matching detection. Multimed Tools Appl 79(41):30709–30733
32. Yoo JC, Han TH (2009) Fast normalized cross-correlation. Circuits Syst Signal Process 28(6):819–843
33. Zear A, Singh PK (2021) Secure and robust color image dual watermarking based on LWT-DCT-SVD. Multimed Tools Appl 1–18
34. Zhang B, Duan H (2017)Three-dimensional path planning for uninhabited combat aerial vehicle based on predator-prey pigeon-inspired optimization in dynamic environment. IEEE/ACM Trans Comput Biol Bioinform 14(1):97–107
35. Zhang X, Zhang W, Sun W, Xu T, Jha SK (2020) A robust watermarking scheme based on ROI and IWT for remote consultation of COVID-19. CMC-Comput Mater Contin 1435–1452